

## Methane Activation by Titanium Monoxide Molecules: A Matrix Isolation Infrared Spectroscopic and Theoretical Study

Guanjun Wang, Yu Gong, Mohua Chen, and Mingfei Zhou\*

Contribution from the Department of Chemistry & Laser Chemistry Institute, Shanghai Key Laboratory of Molecular Catalysts and Innovative Materials, Fudan University, Shanghai 200433, People's Republic of China

Received January 18, 2006; E-mail: mfzhou@fudan.edu.cn

**Abstract:** Reactions of titanium monoxides with methane have been investigated using matrix isolation infrared spectroscopy and theoretical calculations. Titanium derivatives of several simple oxyhydrocarbons have been prepared and identified. The titanium monoxide molecules prepared by laser evaporation of bulk TiO<sub>2</sub> target reacted with methane to form the TiO(CH<sub>4</sub>) complex in solid argon, which was predicted to have C<sub>3v</sub> symmetry with the oxygen atom coordinated to one hydrogen atom of the methane molecule. The complex rearranged to the CH<sub>3</sub>Ti(O)H titano-acetaldehyde molecule upon visible ( $\lambda > 500$  nm) irradiation. The titano-acetaldehyde molecule sustained further photochemical rearrangement to the CH<sub>2</sub>-Ti(H)OH titano-vinyl alcohol molecule, which was characterized to be a simple carbene complex involving agostic bonding. The CH<sub>2</sub>Ti(H)OH molecule reacted with a second methane to form the (CH<sub>3</sub>)<sub>2</sub>Ti(H)OH titano-isopropyl alcohol molecule spontaneously on annealing. The (CH<sub>3</sub>)<sub>2</sub>Ti(H)OH molecule also can be produced via UV photon-induced rearrangement of the CH<sub>3</sub>Ti(O)H(CH<sub>4</sub>) complex.

### Introduction

The selective transformation of ubiquitous but inert C–H bonds of alkanes such as methane to other functional groups is of great economic and scientific importance. Many examples of C–H bond activation at transition-metal centers have been reported.<sup>1–4</sup> To develop practical alkane conversion processes, much remains to be learned about the processes and factors controlling the activity and selectivity of catalytic alkane activation. Reactions of transition-metal atoms and simple metal oxides with methane serve as the simplest model in understanding the intrinsic mechanism of the catalytic alkane conversion processes.

Previous investigations on reactions between transition-metal atoms and methane have shown that insertion into the C–H bond of methane is more facile for metal cations than for neutral metal atoms.<sup>5–10</sup> Transition-metal cations such as zirconium, tantalum, iridium, and platinum all reacted with methane at thermal energies, whereas only neutral platinum atom activated the C–H bond of methane from a gas-phase kinetics study.<sup>10</sup>

Theoretical and matrix isolation experimental investigations suggested that only the neutral rhodium atom is able to activate the C–H bond of methane.<sup>11,12</sup> All of the other transition-metal atoms either are unreactive toward methane or undergo oxidative insertion to form the HMCH<sub>3</sub> species when the metal atom is electronically excited in low-temperature matrixes.<sup>13–17</sup> Recent investigations also showed that the HMCH<sub>3</sub> molecules can undergo further photon-induced rearrangement to form the agostic CH<sub>2</sub>=MH<sub>2</sub> methyldene complexes (group IV metals)<sup>18–20</sup> and CH≡MH<sub>3</sub> methylidyne molecules (Mo and W).<sup>21</sup>

The reactivity of simple transition-metal oxide cations such as monoxide and dioxide cations with methane also has been widely studied in the gas phase.<sup>22–30</sup> The results indicated that

- (1) (a) Janowicz, A. H.; Bergman, R. G. *J. Am. Chem. Soc.* **1982**, *104*, 352. (b) Arndtsen, B. A.; Bergman, R. G.; Mobley, T. A.; Peterson, T. H. *Acc. Chem. Res.* **1995**, *28*, 154.
- (2) Shilov, A. E.; Shul'pin, G. B. *Chem. Rev.* **1997**, *97*, 2879.
- (3) Labinger, J. A.; Bercaw, J. E. *Nature* **2002**, *417*, 507.
- (4) Davies, H. M. L.; Beckwith, R. E. *J. Chem. Rev.* **2003**, *103*, 2861.
- (5) Irikura, K. K.; Beauchamp, J. L. *J. Am. Chem. Soc.* **1991**, *113*, 2769.
- (6) Ranashinge, Y. A.; MacMahon, T. J.; Freiser, B. S. *J. Phys. Chem.* **1991**, *95*, 7721.
- (7) Zhang, X. G.; Liyanage, R.; Armentrout, P. B. *J. Am. Chem. Soc.* **2001**, *123*, 5563.
- (8) Schwarz, H. *Angew. Chem., Int. Ed.* **2003**, *42*, 4442.
- (9) van Koppen, P. A. M.; Perry, J. K.; Kemper, P. R.; Bushnell, J. E.; Bowers, M. T. *Int. J. Mass Spectrom.* **1999**, *185/186/187*, 989.
- (10) Carroll, J. J.; Haug, K. L.; Weisshaar, J. C.; Blomberg, M. R. A.; Siegbahn, P. E. M.; Svensson, M. *J. Phys. Chem.* **1995**, *99*, 13955.

- (11) (a) Blomberg, M. R. A.; Siegbahn, P. E. M.; Svensson, M. *J. Am. Chem. Soc.* **1992**, *114*, 6095. (b) Wittborn, A. M. C.; Costas, M.; Blomberg, M. R. A.; Siegbahn, P. E. M. *J. Chem. Phys.* **1997**, *107*, 4318.
- (12) Wang, G. J.; Chen, M. H.; Zhou, M. F. *Chem. Phys. Lett.* **2005**, *412*, 46.
- (13) (a) Billups, W. E.; Konarski, M. M.; Hauge, R. H.; Margrave, J. L. *J. Am. Chem. Soc.* **1980**, *102*, 7393. (b) Chang, S. C.; Hauge, R. H.; Billups, W. E.; Kafafi, Z. H.; Margrave, J. L. *Inorg. Chem.* **1988**, *27*, 205. (c) Billups, W. E.; Chang, S. C.; Hauge, R. H.; Margrave, J. L. *J. Am. Chem. Soc.* **1993**, *115*, 2039. (d) Billups, W. E.; Chang, S. C.; Hauge, R. H.; Margrave, J. L. *J. Am. Chem. Soc.* **1995**, *117*, 1387.
- (14) (a) Ozin, G. A.; McIntosh, D. F.; Mitchell, S. A. *J. Am. Chem. Soc.* **1981**, *103*, 1574. (b) Ozin, G. A.; McCaffrey, J. G.; Parnis, J. M. *Angew. Chem., Int. Ed. Engl.* **1986**, *25*, 1072.
- (15) Greene, T. M.; Andrews, L.; Downs, A. J. *J. Am. Chem. Soc.* **1995**, *117*, 8180.
- (16) (a) Legay-Sommaire, N.; Legay, F. *Chem. Phys. Lett.* **1994**, *217*, 97. (b) Legay-Sommaire, N.; Legay, F. *Chem. Phys. Lett.* **1996**, *211*, 367.
- (17) (a) Bihlmeier, A.; Greene, T. M.; Himmel, H. J. *Organometallics* **2004**, *23*, 2350. (b) Himmel, H. J. *Chem. Eur. J.* **2004**, *10*, 2851.
- (18) (a) Andrews, L.; Cho, H. G.; Wang, X. F. *Angew. Chem., Int. Ed.* **2005**, *44*, 113. (b) Cho, H. G.; Wang, X. F.; Andrews, L. *J. Am. Chem. Soc.* **2005**, *127*, 465.
- (19) Cho, H. G.; Wang, X. F.; Andrews, L. *Organometallics* **2005**, *24*, 2854.
- (20) Andrews, L.; Cho, H. G.; Wang, X. F. *Inorg. Chem.* **2005**, *44*, 4834.
- (21) (a) Cho, H. G.; Andrews, L. *J. Am. Chem. Soc.* **2005**, *127*, 8226. (b) Cho, H. G.; Andrews, L.; Marsden, C. *Inorg. Chem.* **2005**, *44*, 7634.
- (22) Kappes, M. M.; Staley, R. H. *J. Phys. Chem.* **1981**, *85*, 942.

late transition-metal monoxide ions of the first row can efficiently convert methane to methanol, while the early transition-metal monoxide ions cannot; most dioxide cations are found to be more reactive than the corresponding bare metal cations and monoxide cations. By contrast, reactions of neutral transition-metal oxides with methane have received much less attention. Some theoretical calculations on methane activation by neutral transition-metal oxide molecules ScO, NiO, PdO, and  $\text{MO}_x$  ( $M = \text{Cr}, \text{Mo}, \text{W}$ , and  $x = 1-3$ ) have been reported,<sup>31,32</sup> which have provided valuable information concerning the reaction mechanism and energetics. More recently, reactions of monoxides such as FeO, MnO, NbO, and TaO with methane have been investigated in this laboratory using matrix isolation infrared absorption spectroscopy as well as theoretical calculations.<sup>33,34</sup> It was found that the monoxide molecules reacted with methane to form the weakly bound complexes, which underwent photon-induced rearrangement to the  $\text{CH}_3\text{-MOH}$  ( $M = \text{Fe}, \text{Mn}$ ) or  $\text{CH}_3\text{M}(\text{O})\text{H}$  ( $M = \text{Nb}, \text{Ta}$ ) molecules. In this paper we report a combined matrix isolation infrared spectroscopic and theoretical study of the reaction of titanium monoxide with methane, which provides a prototype reaction in understanding the mechanism of methane activation by transition-metal oxides.

### Experimental and Theoretical Methods

The experimental setup for pulsed laser evaporation and matrix isolation infrared spectroscopic investigation has been described in detail previously.<sup>35</sup> Briefly, the 1064 nm Nd:YAG laser fundamental (Spectra Physics, DCR 150, 20 Hz repetition rate and 8 ns pulse width) was focused onto the rotating Ti or  $\text{TiO}_2$  target. The  $\text{TiO}_2$  target was prepared by sintered titanium dioxide powders. The ablated species were co-deposited with reagent gas in excess argon onto a 12 K CsI window for 1–3 h at a rate of approximately 4 mmol/h. Isotopic labeled  $\text{CD}_4$  (Isotec, 99%),  $^{13}\text{CH}_4$  (Isotec, 99%), and  $\text{CH}_3^{18}\text{OH}$  (Isotec, 99%) were used in different experiments. Infrared spectra were recorded on a Bruker IFS 113 V spectrometer at  $0.5\text{ cm}^{-1}$  resolution using a DTGS detector. Matrix samples were annealed at different temperatures, and selected samples were subjected to broadband irradiation using a tungsten lamp or a high-pressure mercury arc lamp with glass filters.

- (23) Jackson, T. C.; Jacobson, D. B.; Freiser, B. S. *J. Am. Chem. Soc.* **1984**, *106*, 1252.  
 (24) (a) Schröder, D.; Schwarz, H. *Angew. Chem., Int. Ed.* **1995**, *34*, 1973. (b) Schröder, D.; Fiedler, A.; Hrusak, J.; Schwarz, H. *J. Am. Chem. Soc.* **1992**, *114*, 1215. (c) Ryan, M. F.; Fiedler, A.; Schröder, D.; Schwarz, H. *J. Am. Chem. Soc.* **1995**, *117*, 2033. (d) Ryan, M. F.; Fiedler, A.; Schröder, D.; Schwarz, H. *Organometallics* **1994**, *13*, 4072.  
 (25) (a) Clemmer, D. E.; Aristov, N.; Armentrout, P. B. *J. Phys. Chem.* **1993**, *97*, 544. (b) Chen, Y. M.; Clemmer, D. E.; Armentrout, P. B. *J. Am. Chem. Soc.* **1994**, *116*, 7815.  
 (26) Aguirre, F.; Husband, J.; Thompson, C. J.; Stringer, K. L.; Metz, R. B. *J. Chem. Phys.* **2002**, *116*, 4071.  
 (27) Irikura, K. K.; Beauchamp, J. L. *J. Am. Chem. Soc.* **1989**, *111*, 75.  
 (28) Cassidy, C. J.; McElvany, S. W. *Organometallics* **1992**, *11*, 2367.  
 (29) Pope, R. M.; VanOrdan, S. L.; Cooper, B. T.; Buckner, S. W. *Organometallics* **1992**, *11*, 2001.  
 (30) (a) Schröder, D.; Fiedler, A.; Schwarz, J.; Schwarz, H. *Inorg. Chem.* **1994**, *33*, 5094. (b) Wesendrup, R.; Schwarz, H. *Angew. Chem., Int. Ed.* **1995**, *34*, 2033. (c) Fiedler, A.; Kretzschmar, I.; Schröder, D.; Schwarz, H. *J. Am. Chem. Soc.* **1996**, *118*, 9941. (d) Kretzschmar, I.; Fiedler, A.; Harvey, J. N.; Schröder, D.; Schwarz, H. *J. Phys. Chem. A* **1997**, *101*, 6252. (e) Harvey, J. N.; Diefenbach, M.; Schröder, D.; Schwarz, H. *Int. J. Mass Spectrom.* **1999**, *183*, 85. (f) Bronstrup, M.; Schröder, D.; Kretzschmar, I.; Schwarz, H.; Harvey, J. N. *J. Am. Chem. Soc.* **2001**, *123*, 142.  
 (31) (a) Hwang, D. Y.; Mebel, A. M. *Chem. Phys. Lett.* **2002**, *365*, 140. (b) Hwang, D. Y.; Mebel, A. M. *J. Phys. Chem. A* **2002**, *106*, 12072.  
 (32) Xu, X.; Faglioni, F.; Goddard, W. A., III *J. Phys. Chem. A* **2002**, *106*, 7171.  
 (33) Wang, G. J.; Chen, M. H.; Zhou, M. F. *J. Phys. Chem. A* **2004**, *108*, 11273.  
 (34) Wang, G. J.; Lai, S. X.; Chen, M. H.; Zhou, M. F. *J. Phys. Chem. A* **2005**, *109*, 9514.  
 (35) (a) Chen, M. H.; Wang, X. F.; Zhang, L. N.; Yu, M.; Qin, Q. *Z. Chem. Phys.* **1999**, *242*, 81. (b) Zhou, M. F.; Zhang, L. N.; Shao, L. M.; Wang, W. N.; Fan, K. N.; Qin, Q. *Z. J. Phys. Chem. A* **2001**, *105*, 10747. (c) Zhou, M. F.; Zhang, L. N.; Qin, Q. *Z. J. Phys. Chem. A* **2001**, *105*, 6407.

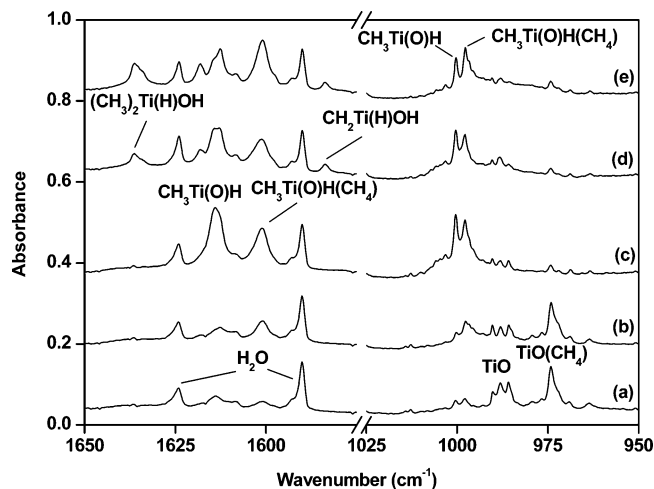


**Figure 1.** Infrared spectra in the 1650–1575 and 1025–950  $\text{cm}^{-1}$  regions from co-deposition of laser-evaporated  $\text{TiO}$  with 5.0%  $\text{CH}_4$  in argon: (a) after 3 h of sample deposition at 12 K, (b) after 30 K annealing, (c) after 30 min of  $\lambda > 500\text{ nm}$  irradiation, (d) after 30 min of  $\lambda > 250\text{ nm}$  irradiation, and (e) after 35 K annealing.

Density functional calculations were performed using the Gaussian 03 program.<sup>36</sup> The three-parameter hybrid functional according to Becke with additional correlation corrections due to Lee, Yang, and Parr (B3LYP) was utilized.<sup>37</sup> The 6-311++G(3df, 3pd) basis set was used for the H, C, Ti, and O atoms.<sup>38</sup> Recent studies have shown that this hybrid DFT functional with a relatively large basis set can provide a very reliable prediction for agostic bonding.<sup>39</sup> The geometries were fully optimized, and the stability of the electronic wave function was tested; the harmonic vibrational frequencies were calculated with analytic second derivatives, and zero-point energies (ZPE) were derived. The single-point energies of all structures optimized at the B3LYP level were calculated using the CCSD(T) method with the 6-311++G(d,p) basis sets.<sup>40</sup>

### Results and Discussion

**Infrared Spectra.** The titanium monoxide reactant was prepared from pulsed laser evaporation of bulk  $\text{TiO}_2$  target. Under controlled laser energy, co-condensation of the species from laser evaporation of  $\text{TiO}_2$  with pure argon at 12 K produced strong titanium monoxide ( $990.3, 988.1,$  and  $985.7\text{ cm}^{-1}$ ) and dioxide absorptions ( $^{48}\text{TiO}_2$ :  $\nu_1, 917.0\text{ cm}^{-1}$  and  $\nu_3, 946.9\text{ cm}^{-1}$ ).<sup>41</sup> These absorptions showed no obvious change upon annealing and broadband irradiation. Distinct new product absorptions were observed in the experiments when different concentration  $\text{CH}_4/\text{Ar}$  mixtures (ranging from 0.2% to 5%) were used as the reagent gas. Figures 1 and 2 show the representative spectra in selected regions with a  $\text{CH}_4/\text{Ar}$  sample (5.0% molar ratio), and the product absorptions are listed in Table 1. Besides the aforementioned titanium oxide absorptions, new absorptions at  $974.1$  and  $1285.8\text{ cm}^{-1}$  were observed after sample deposition at 12 K. These absorptions disappeared when the matrix was irradiated by the output of a tungsten lamp with a  $\lambda > 500\text{ nm}$

- (36) Frisch, M. J. et al. *Gaussian 03*, revision B.05; Gaussian, Inc.: Pittsburgh, PA, 2003.  
 (37) (a) Becke, A. D. *J. Chem. Phys.* **1993**, *98*, 5648. (b) Lee, C.; Yang, E.; Parr, R. G. *Phys. Rev. B* **1988**, *37*, 785.  
 (38) (a) McLean, A. D.; Chandler, G. S. *J. Chem. Phys.* **1980**, *72*, 5639. (b) Krishnan, R.; Binkley, J. S.; Seeger, R.; Pople, J. A. *J. Chem. Phys.* **1980**, *72*, 650.  
 (39) von Frantzius, G.; Streubel, R.; Brandhorst, K.; Grunenberg, J. *Organometallics* **2006**, *25*, 118.  
 (40) Pople, J. A.; Gordon, M. H.; Raghavachari, K. *J. Chem. Phys.* **1987**, *87*, 5968.  
 (41) Chertihin, G. V.; Andrews, L. *J. Phys. Chem.* **1995**, *99*, 6356.

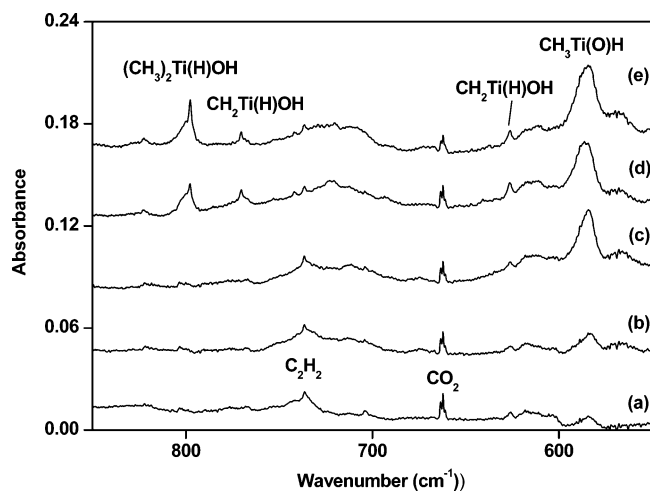


**Figure 2.** Infrared spectra in the 850–550  $\text{cm}^{-1}$  region from co-deposition of laser-evaporated TiO with 5.0%  $\text{CH}_4$  in argon: (a) after 3 h of sample deposition at 12 K, (b) after 30 K annealing, (c) after 30 min of  $\lambda > 500$  nm irradiation, (d) after 30 min of  $\lambda > 250$  nm irradiation, and (e) after 35 K annealing.

pass filter ( $500 < \lambda < 1000$  nm), during which absorptions at 1613.9, 1600.9, 1000.4, 997.9, 583.7, and 474.7  $\text{cm}^{-1}$  were produced. Additional irradiation with the mercury arc lamp without filter ( $250 < \lambda < 580$  nm) decreased the 1613.9, 1600.9, 1000.4, 997.9, 583.7, and 474.7  $\text{cm}^{-1}$  absorptions and produced new absorptions at 3749.0, 3726.7, 1635.8, 1583.8, 797.8, 770.4, and 626.2  $\text{cm}^{-1}$ . The 3726.7, 1613.9, 1583.8, 1000.4, 770.4, and 626.2  $\text{cm}^{-1}$  absorptions decreased, whereas the 3749.0, 1635.8, 1600.9, 997.9, and 797.8  $\text{cm}^{-1}$  absorptions increased upon sample annealing to 35 K. The experiments were repeated with the isotopic labeled  $\text{CD}_4$ ,  $^{13}\text{CH}_4$ , and  $^{12}\text{CH}_4 + ^{13}\text{CH}_4$  samples to help with product identification. The isotopic frequencies are also listed in Table 1. Infrared spectra in selected regions using different isotopic samples are shown in Figures 3 and 4.

Several experiments were done by depositing methanol in argon (0.2%) with laser-evaporated titanium atoms. The spectra in the 1635–1575 and 1050–950  $\text{cm}^{-1}$  regions are shown in Figure 5. The 1613.9, 1583.8, and 1000.4  $\text{cm}^{-1}$  absorptions were produced upon  $300 < \lambda < 580$  nm irradiation. The 1583.8  $\text{cm}^{-1}$  band increased whereas the 1613.9 and 1000.4  $\text{cm}^{-1}$  bands decreased on  $250 < \lambda < 580$  nm irradiation. The 1583.8  $\text{cm}^{-1}$  band exhibited no shift, while the 1613.9 and 1000.4  $\text{cm}^{-1}$  absorptions were shifted to 1613.2 and 959.3  $\text{cm}^{-1}$  with the  $\text{CH}_3^{18}\text{OH}$  sample (Figure 5, trace d).

**TiO( $\text{CH}_4$ ).** The 974.1  $\text{cm}^{-1}$  absorption, which shows no carbon-13 isotopic shift and a small (6.4  $\text{cm}^{-1}$ ) deuterium shift, is assigned to the  $\text{TiO}(\text{CH}_4)$  complex. This absorption is barely observed in the experiment when laser-evaporated titanium atoms were co-deposited with  $\text{O}_2/\text{CH}_4$  mixture, in which the TiO absorption is very weak. The band position also suggests that it is due to the Ti–O stretching mode of a TiO complex. The very weak absorption at 1285.8  $\text{cm}^{-1}$  is the  $\text{CH}_2$  deformation mode of the complex, which shows about the same isotopic frequency shift as that of  $\text{CH}_4$  observed at 1305.4  $\text{cm}^{-1}$ . The  $\text{TiO}(\text{CH}_4)$  complex was predicted to have a  $\text{C}_{3v}$  structure with one H atom of  $\text{CH}_4$  coordinated to the O atom of TiO (Figure 6). The small deformation of the  $\text{CH}_4$  and TiO subunits and the rather long O–H distance (2.658 Å) indicate weak interac-

tion between the  $\text{CH}_4$  and TiO subunits. The binding energy with respect to  $\text{TiO} + \text{CH}_4$  was predicted to be 1.1 kcal/mol at the CCSD(T) level, significantly lower than those of other previously reported transition-metal monoxide–methane complexes, which were predicted to be coordinated between the metal and H atoms.<sup>31–34</sup>

**$\text{CH}_3\text{Ti}(\text{O})\text{H}$  and  $\text{CH}_3\text{Ti}(\text{O})\text{H}(\text{CH}_4)$ .** The absorptions at 1613.9 and 1000.4  $\text{cm}^{-1}$  appeared under  $500 < \lambda < 1000$  nm irradiation at the expense of the  $\text{TiO}(\text{CH}_4)$  absorptions. This observation suggests that the 1613.9 and 1000.4  $\text{cm}^{-1}$  absorptions are most likely due to a structural isomer of  $\text{TiO}(\text{CH}_4)$ . The same absorptions were also observed in the  $\text{Ti} + \text{CH}_3\text{OH}$  experiments. The 1613.9  $\text{cm}^{-1}$  absorption shows no shift with the  $^{13}\text{CH}_4$  sample and shifted to 1165.3  $\text{cm}^{-1}$  with the  $\text{CD}_4$  sample. The band position and the H/D isotope frequency ratio (1.3850) are characteristic of a Ti–H stretching vibration.<sup>42</sup> The absorption at 1000.4  $\text{cm}^{-1}$  exhibits a very small (0.3  $\text{cm}^{-1}$ ) carbon-13 shift and large oxygen-18 (41.1  $\text{cm}^{-1}$ ) shift. The band position and  $^{16}\text{O}/^{18}\text{O}$  isotopic frequency ratio (1.0428) indicate a terminal Ti–O stretching vibration. Accordingly, we assign the 1613.9 and 1000.4  $\text{cm}^{-1}$  absorptions to the  $\text{CH}_3\text{Ti}(\text{O})\text{H}$  molecule. These frequencies are comparable to the 1611.9 (antisymmetric Ti–H stretch) and 1010.5  $\text{cm}^{-1}$  (Ti–O stretch) values for the tetravalent Ti species  $\text{H}_2\text{TiO}$  observed in solid argon.<sup>43</sup>

The absorptions at 1600.9 and 997.9  $\text{cm}^{-1}$  are several wavenumbers red shifted from the Ti–H and Ti–O stretching modes of  $\text{CH}_3\text{Ti}(\text{O})\text{H}$ . The band positions and isotopic frequency shifts indicate that the upper band is due to a Ti–H stretching mode, and the lower band is a Ti–O stretching mode. These absorptions were not observed in the  $\text{Ti} + \text{CH}_3\text{OH}$  experiments. Both absorptions increased together on annealing at the expense of the  $\text{CH}_3\text{Ti}(\text{O})\text{H}$  absorptions, and the relative intensities with respect to the  $\text{CH}_3\text{Ti}(\text{O})\text{H}$  absorptions increased with increasing  $\text{CH}_4$  concentrations. The above-mentioned observations led us to assign these absorptions to the  $\text{CH}_3\text{Ti}(\text{O})\text{H}(\text{CH}_4)$  complex.

The  $\text{CH}_3\text{Ti}(\text{O})\text{H}$  molecule was predicted to have a singlet ground state with a nonplanar  $\text{C}_1$  structure (Figure 6). The calculated Ti–C bond length of 2.088 Å suggests a Ti–C single bond, which is very close to the standard single Ti–C bond lengths in tetraaryl compounds.<sup>44</sup> The  $\text{CH}_3\text{Ti}(\text{O})\text{H}$  molecule can be regarded as a titan–acetaldehyde. The Ti–H and Ti–O stretching modes were computed at 1678.0 and 1064.9  $\text{cm}^{-1}$ , respectively. These two modes were predicted to have the largest IR intensities. The isotopic frequency shifts calculated for both modes fit the experimental values very well (Table 1). The calculations also predicted that  $\text{CH}_3\text{Ti}(\text{O})\text{H}$  may be coordinated by another  $\text{CH}_4$  molecule to form the  $\text{CH}_3\text{Ti}(\text{O})\text{H}(\text{CH}_4)$  complex, which was computed to have  $\eta^3$ - $\text{CH}_4$  bonding, that is, the titanium atom is coordinated by three hydrogen atoms of  $\text{CH}_4$  (Figure 6). The distance between Ti and C is 2.485 Å. The Ti–O, Ti–C, and Ti–H bond lengths of  $\text{CH}_3\text{Ti}(\text{O})\text{H}$  were slightly elongated upon  $\text{CH}_4$  coordination, which induced a red shift of the corresponding vibrational frequencies.

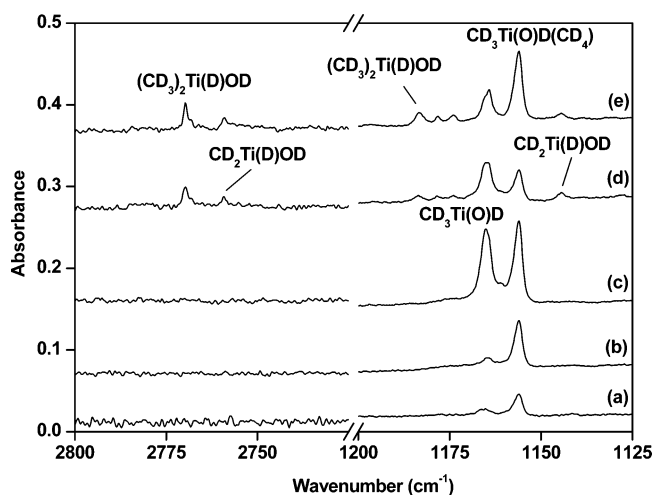
(42) (a) Xiao, Z. L.; Hauge, R. H.; Margrave, J. L. *J. Phys. Chem.* **1991**, *95*, 2696. (b) Chertihin, G. V.; Andrews, L. *J. Am. Chem. Soc.* **1994**, *116*, 8322.

(43) Zhou, M. F.; Zhang, L. N.; Dong, J.; Qin, Q. Z. *J. Am. Chem. Soc.* **2000**, *122*, 10680.

(44) Bassi, I.; Allegra, G.; Scordamaglia, R.; Chiccola, G. *J. Am. Chem. Soc.* **1971**, *93*, 3787.

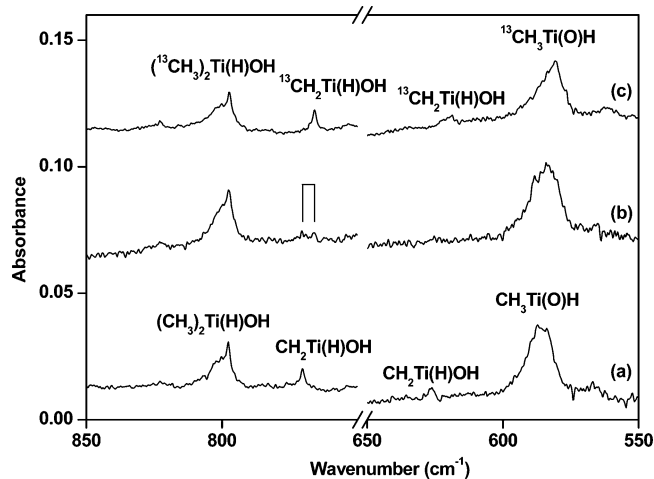
**Table 1.** Infrared Absorptions ( $\text{cm}^{-1}$ ) from Co Deposition of Laser-Evaporated Titanium Oxides with  $\text{CH}_4$  in Solid Argon at 12 K (calculated frequencies are also listed in parentheses for comparison)

$\text{CH}_4$	$^{13}\text{CH}_4$	$\text{CD}_4$	assignment
3749.0 (3934.1)	3749.0 (3934.1)	2782.4 (2867.4)	$(\text{CH}_3)_2\text{Ti}(\text{H})\text{OH}$ (O–H stretch)
3726.7 (3911.5)	3726.7 (3911.5)	2759.3 (2849.4)	$\text{CH}_2\text{Ti}(\text{H})\text{OH}$ (O–H stretch)
1635.8 (1703.5)	1635.8 (1703.5)	1183.7 (1218.8)	$(\text{CH}_3)_2\text{Ti}(\text{H})\text{OH}$ (Ti–H stretch)
1613.9 (1678.0)	1613.9 (1678.0)	1165.3 (1200.9)	$\text{CH}_3\text{Ti}(\text{O})\text{H}$ (Ti–H stretch)
1600.9 (1659.0)	1600.9 (1658.9)	1155.9 (1187.3)	$\text{CH}_3\text{Ti}(\text{O})\text{H}(\text{CH}_4)$ (Ti–H stretch)
1583.8 (1648.7)	1583.8 (1648.7)	1144.6 (1180.2)	$\text{CH}_2\text{Ti}(\text{H})\text{OH}$ (Ti–H stretch)
1285.8 (1334.1)	1278.3 (1325.9)		$\text{TiO}(\text{CH}_4)$ ( $\text{CH}_2$ deformation)
1000.4 (1064.9)	1000.1 (1064.6)		$\text{CH}_3\text{Ti}(\text{O})\text{H}$ (Ti–O stretch)
997.9 (1049.8)	997.6 (1049.6)		$\text{CH}_3\text{Ti}(\text{O})\text{H}(\text{CH}_4)$ (Ti–O stretch)
974.1 (1039.2)	974.1 (1039.2)	967.7 (1039.3)	$\text{TiO}(\text{CH}_4)$ (Ti–O stretch)
797.8 (796.5)	797.4 (796.2)	772.9 (768.8)	$(\text{CH}_3)_2\text{Ti}(\text{H})\text{OH}$ (Ti–OH stretch)
770.4 (761.2)	765.9 (755.6)	733.7 (710.1)	$\text{CH}_2\text{Ti}(\text{H})\text{OH}$ (Ti–OH stretch)
626.2 (669.9)	618.3 (664.0)		$\text{CH}_2\text{Ti}(\text{H})\text{OH}$ ( $\text{CH}_2$ wagging)
583.7 (597.7)	580.3 (595.0)	501.8 (515.6)	$\text{CH}_3\text{Ti}(\text{O})\text{H}$ (HTiO bend + TiC stretch)
583.7 (598.6)	580.3 (596.7)	511.5 (509.1)	$\text{CH}_3\text{Ti}(\text{O})\text{H}(\text{CH}_4)$ (HTiO bend + TiC stretch)
474.7 (496.2)		436.3 (447.2)	$\text{CH}_3\text{Ti}(\text{O})\text{H}$ (HTiO deformation)

**Figure 3.** Infrared spectra in the 2800–2725 and 1200–1125  $\text{cm}^{-1}$  regions from co-deposition of laser-evaporated TiO with 5.0%  $\text{CD}_4$  in argon: (a) after 3 h of sample deposition at 12 K, (b) after 30 K annealing, (c) after 30 min of  $\lambda > 500$  nm irradiation, (d) after 30 min of  $\lambda > 250$  nm irradiation, and (e) after 35 K annealing.

Weak absorption at  $474.7 \text{ cm}^{-1}$  exhibited the same annealing and photolysis behavior as the  $1613.9$  and  $1000.4 \text{ cm}^{-1}$  absorptions and is assigned to the HTiO deformation mode of  $\text{CH}_3\text{Ti}(\text{O})\text{H}$ , which was predicted at  $496.2 \text{ cm}^{-1}$ . A broad band centered at  $583.7 \text{ cm}^{-1}$  tracked with the sum of the  $1613.9$  and  $1600.9 \text{ cm}^{-1}$  absorptions. This band is assigned to the mixed HTiO bending and Ti–C stretching mode of  $\text{CH}_3\text{Ti}(\text{O})\text{H}$  and  $\text{CH}_3\text{Ti}(\text{O})\text{H}(\text{CH}_4)$ , which were predicted at  $597.7 \text{ cm}^{-1}$  for  $\text{CH}_3\text{Ti}(\text{O})\text{H}$  and  $598.6 \text{ cm}^{-1}$  for  $\text{CH}_3\text{Ti}(\text{O})\text{H}(\text{CH}_4)$ .

**$\text{CH}_2\text{Ti}(\text{H})\text{OH}$ .** Weak absorptions at  $3726.7$ ,  $1583.8$ ,  $770.4$ , and  $626.2 \text{ cm}^{-1}$  appeared together on  $250 < \lambda < 580$  nm irradiation, during which the  $\text{CH}_3\text{Ti}(\text{O})\text{H}$  absorptions decreased. The  $3726.7 \text{ cm}^{-1}$  absorption is due to an O–H stretching mode, which shifted to  $2759.3 \text{ cm}^{-1}$  with  $\text{CD}_4$  (H/D ratio 1.3506). The  $1583.8 \text{ cm}^{-1}$  absorption exhibited an H/D isotopic ratio of 1.3837 and is a Ti–H stretching vibration. The  $770.4 \text{ cm}^{-1}$  absorption is largely a Ti–OH stretching mode but with some carbon involvement. It shifted to  $765.9 \text{ cm}^{-1}$  with  $^{13}\text{CH}_4$ , and only the pure isotopic counterparts were observed in the experiment with a mixed  $^{12}\text{CH}_4 + ^{13}\text{CH}_4$  sample (Figure 4). The  $626.2 \text{ cm}^{-1}$  absorption shifted to  $618.3 \text{ cm}^{-1}$  with  $^{13}\text{CH}_4$

**Figure 4.** Infrared spectra in the 850–750 and 650–550  $\text{cm}^{-1}$  regions from co-deposition of laser-evaporated TiO with methane in excess argon. Spectra were taken after 3 h of sample deposition followed by 30 min of  $\lambda > 250$  nm irradiation: (a) 2.0%  $^{12}\text{CH}_4$ , (b) 2.0%  $^{12}\text{CH}_4 + 2.0\%$   $^{13}\text{CH}_4$ , and (c) 2.0%  $^{13}\text{CH}_4$ .

and is due to a  $\text{CH}_2$  wagging vibration. Accordingly, we assign these absorptions to the  $\text{CH}_2\text{Ti}(\text{H})\text{OH}$  molecule.

Our calculations predicted that the  $\text{CH}_2\text{Ti}(\text{H})\text{OH}$  molecule has a singlet ground state with nonplanar  $C_1$  structure, as illustrated in Figure 6. The Ti–C bond length of  $1.815 \text{ \AA}$  is slightly shorter than the experimentally known Ti=C double bond length.<sup>45</sup> The  $\text{CH}_2\text{Ti}(\text{H})\text{OH}$  molecule is a methylenedihydroxo complex, which can also be regarded as a titanovinyl alcohol molecule. Similar to the recently reported methylenedihydroxo  $\text{CH}_2=\text{MH}_2$  and the fluorine-substituted derivatives  $\text{CH}_2=\text{MHF}$  (M = Ti, Zr, Hf, Mo, and W),<sup>18–21,46</sup> the  $\text{CH}_2\text{Ti}(\text{H})\text{OH}$  titanovinyl alcohol molecule also involves agostic interaction between the metal atom and one of the  $\alpha$ -hydrogen atoms.<sup>47</sup> As shown in Figure 6, the methylene group is distorted with one of the methylene hydrogen atoms located close to the Ti atom:  $\angle \text{HCTi} = 89.1^\circ$  and  $r_{\text{CH}\cdots\text{Ti}} = 2.117 \text{ \AA}$ .

(45) (a) Baumann, R.; Stumpf, R.; Davis, W. M.; Liang, L. C.; Schrock, R. R. *J. Am. Chem. Soc.* **1999**, *121*, 7822. (b) Schrock, R. R. *Chem. Rev.* **2002**, *102*, 145.(46) (a) Cho, H. G.; Andrews, L. *J. Am. Chem. Soc.* **2004**, *126*, 10485. (b) Cho, H. G.; Andrews, L. *J. Phys. Chem. A* **2004**, *108*, 6294. (c) Cho, H. G.; Andrews, L. *Organometallics* **2004**, *23*, 4357.(47) Scherer, W.; McGrady, G. S. *Angew. Chem., Int. Ed.* **2004**, *43*, 1782 and references therein.

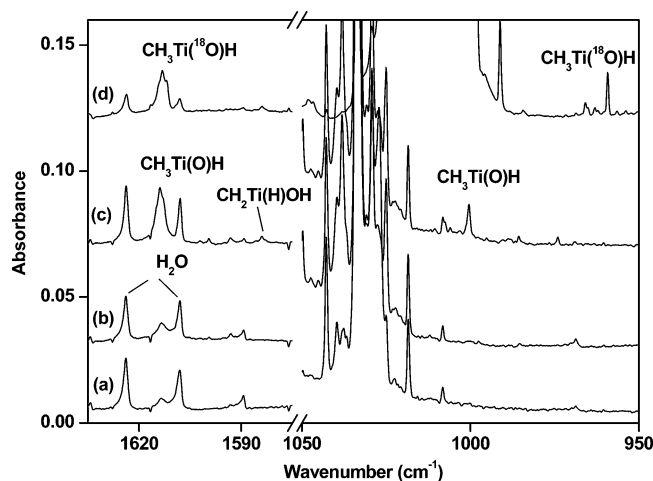


**Figure 5.** Infrared spectra in the 1635–1575 and 1050–950  $\text{cm}^{-1}$  regions from co-deposition of laser-evaporated titanium with  $\text{CH}_3\text{OH}$  in excess argon: (a) 0.2%  $\text{CH}_3\text{OH}$ , 2 h of sample deposition at 12 K, (b) after 25 K annealing of sample a, (c) after 30 min of  $300 < \lambda < 580$  nm irradiation of sample b, and (d) 0.2%  $\text{CH}_3^{18}\text{OH}$ , after 30 min of  $300 < \lambda < 580$  nm irradiation.

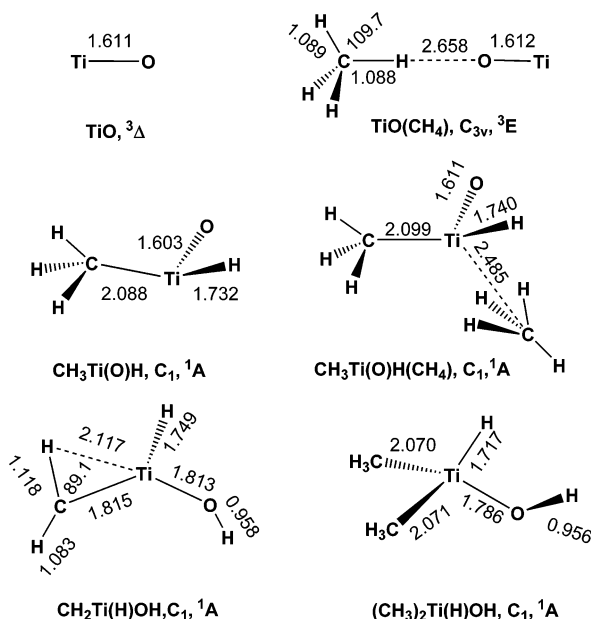
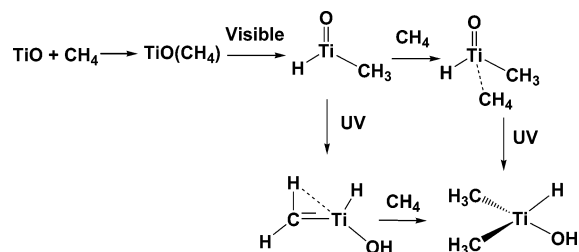


**Figure 6.** Optimized structures (bond lengths in angstroms, bond angles in degrees) of the observed product molecules at the B3LYP/6-311++G-(3df,3pd) level of theory.

The experimentally observed vibrational modes were computed at 3911.5, 1648.7, 761.2, and 669.9  $\text{cm}^{-1}$  with the calculated isotopic shifts in good agreement with the experimental values.

**$(\text{CH}_3)_2\text{Ti}(\text{H})\text{OH}$ .** Absorptions at 3749.0, 1635.8, and 797.8  $\text{cm}^{-1}$  appeared only upon  $250 < \lambda < 580$  nm irradiation and increased on subsequent annealing. High reagent concentration favors production of these absorptions, which suggests involvement of more than one  $\text{CH}_4$ . The 3749.0  $\text{cm}^{-1}$  absorption moved to 2782.4  $\text{cm}^{-1}$  with the  $\text{CD}_4$  sample and is assigned to an O–H stretching vibration. The 1635.8  $\text{cm}^{-1}$  absorption is a Ti–H stretching vibration based upon the observed H/D isotopic frequency ratio of 1.3819. The 797.8  $\text{cm}^{-1}$  absorption shows an isotopic shift of 0.4  $\text{cm}^{-1}$  on carbon-13 substitution and a 24.9  $\text{cm}^{-1}$  shift on  $\text{CD}_4$  substitution. On the basis of the small carbon and deuterium isotopic shifts, the 797.8  $\text{cm}^{-1}$  absorption arises from a vibrational mode such as a Ti–OH stretch where

**Scheme 1**



the O atom is heavily involved. The above considerations suggest the assignment of the 3749.0, 1635.8, and 797.8  $\text{cm}^{-1}$  absorptions to the  $(\text{CH}_3)_2\text{Ti}(\text{H})\text{OH}$  titanol–isopropyl alcohol molecule. Calculations were performed for the  $(\text{CH}_3)_2\text{Ti}(\text{H})\text{OH}$  molecule, which was predicted to have a singlet ground state without symmetry ( $C_1$ , see Figure 6). The H atom of the hydroxyl group tilted from the  $\text{HTiO}$  plane with a dihedral angle of 103.0°. The two Ti–C bonds are slightly different with both bond lengths close to that of  $\text{CH}_3\text{Ti}(\text{O})\text{H}$ . The O–H, Ti–H, and Ti–O stretching modes were predicted to have the largest IR intensities, which absorbed at 3934.1, 1703.5, and 796.5  $\text{cm}^{-1}$ , respectively.

**Reaction Mechanism.** The behavior of the new product absorptions leads us to propose the reactions shown in Scheme 1.

The initial step of the  $\text{TiO} + \text{CH}_4$  reaction is formation of the  $\text{TiO}(\text{CH}_4)$  complex. From the complex one hydrogen atom of methane transferred to the metal center to form the  $\text{CH}_3\text{Ti}(\text{O})\text{H}$  titanol–acetaldehyde molecule. According to the calculations, the singlet ground-state  $\text{CH}_3\text{Ti}(\text{O})\text{H}$  molecule is 6.9 kcal/mol lower in energy than the triplet-state  $\text{TiO}(\text{CH}_4)$  complex. The H-atom transfer process is exothermic but requires activation energy. The barrier height was computed to be 23.3 kcal/mol (Figure 7). This process involves spin crossing and proceeds only under visible light ( $\lambda > 500$  nm) irradiation, during which some excited states may be involved. Another possible reaction channel with hydrogen being transferred to the O atom of  $\text{TiO}$  to form the  $\text{CH}_3\text{TiOH}$  isomer was predicted to be energetically unfavorable. The  $\text{CH}_3\text{TiOH}$  isomer has a triplet ground state, which is 3.7 kcal/mol less stable than the singlet ground-state  $\text{CH}_3\text{Ti}(\text{O})\text{H}$  molecule. No evidence was found for formation of  $\text{CH}_3\text{TiOH}$  in the present experiments. This reaction feature is very similar to those of other early transition metals (Nb and Ta) but is quite different from those of late transition metals (Mn and Fe) as reported previously by our group.<sup>33,34</sup> The  $\text{MnO}(\text{CH}_4)$  and  $\text{FeO}(\text{CH}_4)$  complexes underwent photochemical rearrangement to form the  $\text{CH}_3\text{MnOH}$  and  $\text{CH}_3\text{FeOH}$  molecules instead of  $\text{CH}_3\text{Mn}(\text{O})\text{H}$  and  $\text{CH}_3\text{Fe}(\text{O})\text{H}$  upon UV irradiation.<sup>33</sup> The different reactivity can be rationalized in terms of changes in the strength of the M–O bonds and the electron count. In general, the bonds of early transition-metal monoxides are stronger than those of late transition-metal monoxides (the bond dissociation energies of  $\text{TiO}$ ,  $\text{MnO}$ , and  $\text{FeO}$  are  $6.92 \pm 0.10$ ,  $3.83 \pm 0.08$ , and  $4.17 \pm 0.08$  eV, respectively).<sup>48</sup> The valence d electrons of early transition metals are inclined to participate in bonding to form high-valent compounds, whereas the late

(48) Merer, A. J. *Annu. Rev. Phys. Chem.* **1989**, *40*, 407 and references therein.

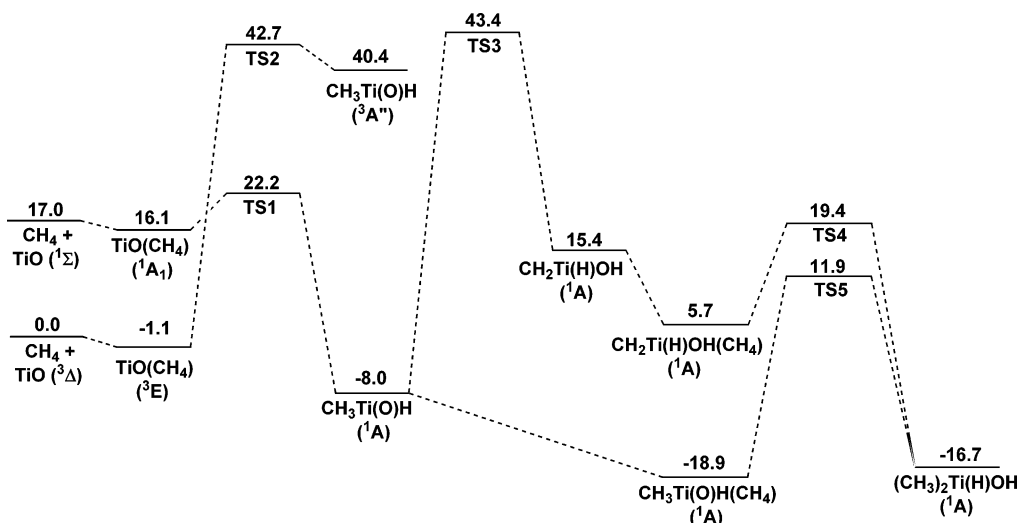


**Figure 7.** Potential-energy profiles for the TiO + CH<sub>4</sub> reaction calculated at the CCSD(T)/6-311++G\*\*/B3LYP/6-311++G (3df, 3pd) level of theory (values are given in kcal/mol).

transition metals Mn and Fe prefer to form divalent molecules due to the stability of the d<sup>5</sup> and d<sup>6</sup> electronic configurations.<sup>49</sup>

Under UV light irradiation one hydrogen atom of the CH<sub>3</sub> group can be transferred further to the O atom in CH<sub>3</sub>Ti(O)H to form the CH<sub>2</sub>Ti(H)OH isomer. The CH<sub>2</sub>Ti(H)OH structure is 23.4 kcal/mol less stable than the ground-state CH<sub>3</sub>Ti(O)H isomer. The reaction on the singlet ground state was computed to proceed via a transition state (TS3) lying 51.4 kcal/mol above CH<sub>3</sub>Ti(O)H (Figure 7). A similar UV-induced α-H transfer has been observed for CH<sub>3</sub>TiX to form CH<sub>2</sub>TiHX (X = H, F) in reactions of Ti atoms with CH<sub>4</sub> and CH<sub>3</sub>F.<sup>20,46b</sup>

Upon sample annealing, the CH<sub>2</sub>Ti(H)OH titano–vinyl alcohol absorptions decreased while the (CH<sub>3</sub>)<sub>2</sub>Ti(H)OH titano–isopropyl alcohol absorptions increased. This implies that CH<sub>2</sub>Ti(H)OH activates a second methane with very low activation energy. As shown in Figure 7, the activation process is exothermic by about 32.1 kcal/mol. The reaction proceeds with initial formation of a CH<sub>2</sub>Ti(H)OH(CH<sub>4</sub>) complex followed by a hydrogen-atom transfer via a transition state (TS4) lying 4.0 kcal/mol above the CH<sub>2</sub>Ti(H)OH + CH<sub>4</sub> reactants. The energy barrier is quite low, and tunneling effects, which are common for hydrogen-atom transfer reactions, might be responsible for formation of (CH<sub>3</sub>)<sub>2</sub>Ti(H)OH on annealing.<sup>50</sup> This reaction is analogous to that for CH<sub>2</sub>TiH<sub>2</sub> and CH<sub>4</sub> to form the simple titano–propane (CH<sub>3</sub>)<sub>2</sub>TiH<sub>2</sub> molecule.<sup>20</sup>

The CH<sub>3</sub>Ti(O)H molecule reacted with CH<sub>4</sub> to form the CH<sub>3</sub>Ti(O)H(CH<sub>4</sub>) complex on annealing. This complex was predicted to be bound by 10.9 kcal/mol with respect to CH<sub>3</sub>Ti(O)H and CH<sub>4</sub>. The complex also rearranged to (CH<sub>3</sub>)<sub>2</sub>Ti(H)OH under UV light irradiation. The (CH<sub>3</sub>)<sub>2</sub>Ti(H)OH molecule is 2.2 kcal/mol less stable than the complex. The reaction from CH<sub>3</sub>Ti(O)H(CH<sub>4</sub>) to (CH<sub>3</sub>)<sub>2</sub>Ti(H)OH on the singlet ground state was computed to proceed via a transition state (TS5) lying 30.8 kcal/mol above the complex (Figure 7).

Laser evaporation of bulk TiO<sub>2</sub> target produces TiO as well as TiO<sub>2</sub>. Theoretical calculations indicated that TiO<sub>2</sub> can also

form a stable complex with CH<sub>4</sub> with a binding energy of 9.4 kcal/mol (see Supporting Information). However, no product due to the TiO<sub>2</sub> + CH<sub>4</sub> reaction was observed in the present experiments. Recent studies in our laboratory have shown that early transition-metal monoxides trapped in solid argon do not form stable complexes with argon; however, the dioxide molecules are coordinated by argon atoms with relatively strong metal–Ar binding energies.<sup>51</sup> Quantum chemical calculations indicated that TiO<sub>2</sub> could coordinate two argon atoms. The TiO<sub>2</sub>(Ar)<sub>2</sub> complexes have a <sup>1</sup>A<sub>1</sub> ground state with C<sub>2v</sub> symmetry (see Supporting Information). The total Ti–Ar binding energy was predicted to be 10.9 kcal/mol, ca. 1.5 kcal/mol larger than that of the TiO<sub>2</sub>(CH<sub>4</sub>) complex calculated at the same level of theory. Therefore, the TiO<sub>2</sub> absorptions observed in solid argon should be regarded as the TiO<sub>2</sub>(Ar)<sub>2</sub> complex isolated in solid argon matrix; the TiO<sub>2</sub>(CH<sub>4</sub>) complex cannot be formed via TiO<sub>2</sub>(Ar)<sub>2</sub> + CH<sub>4</sub> reaction. In contrast, calculations on TiO(Ar) almost converged to separated TiO and Ar (Ti–Ar distance larger than 6 Å) with negligible binding energy, which indicated that TiO does not form a complex with Ar.

## Conclusions

Methane activation by titanium monoxide molecules has been investigated using matrix isolation infrared spectroscopy and theoretical calculations. The titanium monoxide molecules prepared by laser evaporation of bulk TiO<sub>2</sub> target reacted with methane to form the TiO(CH<sub>4</sub>) complex. The complex rearranged to the CH<sub>3</sub>Ti(O)H titano–acetaldehyde molecule upon visible (λ > 500 nm) irradiation. The titano–acetaldehyde molecule sustained further photon-induced α-hydrogen transfer to give the CH<sub>2</sub>Ti(H)OH titano–vinyl alcohol molecule, which was characterized to be a simple carbene complex involving agostic bonding. A second methane activation occurred to form the (CH<sub>3</sub>)<sub>2</sub>Ti(H)OH titano–isopropyl alcohol spontaneously on annealing. The (CH<sub>3</sub>)<sub>2</sub>Ti(H)OH molecule also can be produced via UV photon-induced rearrangement of the CH<sub>3</sub>Ti(O)H(CH<sub>4</sub>) complex. These molecules are identified by isotopic substitution and comparison to DFT frequency calculations. As shown in

(49) (a) Zhou, M. F.; Zhang, L. N.; Shao, L. M.; Wang, W. N.; Fan, K. N.; Qin, Q. Z. *J. Phys. Chem. A* **2001**, *105*, 5801. (b) Zhang, L. N.; Zhou, M. F.; Shao, L. M.; Wang, W. N.; Fan, K. N.; Qin, Q. Z. *J. Phys. Chem. A* **2001**, *105*, 6998.

(50) (a) Pettersson, M.; Macoas, E. M. S.; Khriachtchev, L.; Lundell, J.; Fausto, R.; Rasanen, M. *J. Chem. Phys.* **2002**, *117*, 9095. (b) Espinosa-Garcia, J.; Corchado, J. C.; Truhlar, D. G. *J. Am. Chem. Soc.* **1997**, *119*, 9891.

(51) (a) Zhao, Y. Y.; Wang, G. J.; Chen, M. H.; Zhou, M. F. *J. Phys. Chem. A* **2005**, *109*, 6621. (b) Zhao, Y. Y.; Gong, Y.; Chen, M. H.; Ding, C. F.; Zhou, M. F. *J. Phys. Chem. A* **2005**, *109*, 11765. (c) Zhao, Y. Y.; Gong, Y.; Chen, M. H.; Zhou, M. F. *J. Phys. Chem. A* **2006**, *110*, 1845.

this study, the  $\text{TiO} + \text{CH}_4$  reaction may serve as a model system in understanding the intrinsic mechanism of transition-metal-mediated alkane conversion.

**Acknowledgment.** We thank Dr. Qiang Xu for helpful discussions. This work was supported by the NKBRF of China (2004CB719501).

**Supporting Information Available:** Complete ref 36 and absolute energies, vibrational frequencies and intensities, and geometries (as Cartesian coordinates) of all calculated structures. This material is available free of charge via the Internet at <http://pubs.acs.org>.

JA0604010